ELECTROCHEMICAL INVESTIGATION OF INHIBITORY OF NEW SYNTHESIZED TETRAZOLE DERIVATIVE ON CORROSION OF STAINLESS STEEL 316L IN ACIDIC MEDIUM

A. Ehsani[1,2*], Sh. Bodaghi[2], H. Mohammad Shiri[2], H. Mostaanzadeh[1] and M. Hadi[1]

* *ehsani46847@yahoo.com*

Received: August 2015 **Accepted: August 2016**

[1] Department of Chemistry, Faculty of science, University of Qom, Qom, Iran.
[2] Department of Chemistry, Payame Noor University, Iran.

Abstract: *In this study, an organic compound inhibitor, namely N-benzyl-N-(4-chlorophenyl)-1H-tetrazole-5-amine (NBTA), was synthesized and the role of this inhibitor for corrosion protection of stainless steel (SS) exposed to 0.5 M H2SO4 was investigated using electrochemical, and quantum analysis. By taking advantage of potentiodynamic polarization, the inhibitory action of NBTA was found to be mainly mixed type with dominant anodic inhibition. The effectiveness of the inhibitor was also indicated using electrochemical impedance spectroscopy (EIS). Moreover, to provide further insight into the mechanism of inhibition, quantum chemical calculations of the inhibitor were performed. The adsorption of NBTA onto the SS surface followed the Langmuir adsorption model with the free energy of adsorption ΔG0ads of of -7.88 kJ mol-1. Quantum chemical calculations were employed to give further insight into the mechanism of inhibition action of NBTA.*

Keywords: *organic inhibitor, adsorption, stainless steel, impedance, Density functional theory.*

1. INTRODUCTION

Since iron and its alloys are the backbone of industrial constructions, many research projects have been concerned with their stability. One of most important tasks is the retardation of the attack by acid solutions used during pickling, industrial cleaning and descaling. The use of an additive is one of the major solutions for this problem. Hence, various additives are used to protect iron and its alloy against corrosive attack. A variety of organic compounds, particularly azole derivatives containing heteroatoms such as nitrogen and sulphur, aromatic rings and π bonds has been already examined to inhibit the corrosion of metals [1-6]. The existing data show that organic inhibitors act by adsorption and they protect the metal by film formation. Organic compounds bearing heteroatoms with high electron density such as phosphorus, sulfur, nitrogen, oxygen or those containing multiple bonds which are considered as adsorption centers, are effective as corrosion inhibitors [6-10]. The compounds containing both nitrogen and sulfur in their molecular structure have exhibited greater inhibition compared with those possessing only one of these atoms [11-13]. In the literature, many thiazole derivatives [14-16] have been reported as corrosion inhibitors and found to have good corrosion inhibition effect. The efficiency of an organic compound inhibitor is mainly dependent on its ability to adsorb on a metal surface, which consists of replacement of a water molecule at a corroding interface. The present work aims to evaluate the inhibitory effect of new synthesized NBTA on the steel corrosion in acidic solution. Different aspects of electrochemical measurements, including potentiodynamic polarization and electrochemical impedance spectroscopy, were used to study the inhibition mechanism of the inhibitor. Moreover, to provide further insight into the mechanism of inhibition, quantum chemical calculations of the inhibitor based on DFT method were performed.

2. EXPERIMENTAL

2. 1. Materials and Apparatus

Stainless steel 316L has the composition (wt %) Fe: 67.95, Ni: 10.60, Si: 0.45, Mn: 1.75, Cr: 16.50, S: 0.025, P: 0.028, Mo: 2.10, Al: 0.008, Co: 0.16, Cu: 0.35, Nb: 0.01 and V: 0.02. The

[DOI: 10.22068/ijmse.13.3.19]

exposed surface of the SS electrode was ground with silicon carbide abrasive paper from 400 to 1200, degreased with absolute ethanol, rinsed in distilled water, and dried in warm air. The corrosive medium was 0.5 M H_2SO_4 solution prepared from analytical reagent grade 98% sulfuric acid and distilled water. For synthesizing the organic inhibitor, a mixture of N-benzyl-N-(4-chlorophenyl) cyanamide, sodium azide and $ZnCl_2$/$AlCl_3$/Silica in distilled DMF was heated up to 120 °C for 3h and stirred under ultrasonic irradiation.

The concentration range of inhibitor employed was 10-4 to 10-3 M in 0.5 M sulfuric acid. All electrochemical measurements were carried out in a conventional three electrode cell, powered by a potentiostat/galvanostat (EG&G 273A) and a frequency response analyzer (EG&G, 1025). The system was run by a PC through M270 and M398 software via a GPIB interface. The frequency range of 100 kHz to 15 mHz and modulation amplitude of 5 mV were employed for impedance studies. A SS electrode was employed as the working electrode. A saturated calomel electrode (SCE) and a platinum wire were used as reference and counter electrodes, respectively. Before measurement, the working electrode was immersed in test solution for approximately 1 h until a steady open circuit potential (OCP) was reached. The polarization curves were carried out from cathodic potential of -1.4 V to anodic potential of 0.10 V with respect to the open circuit potential at a sweep rate of 0.5 mV/s. The linear Tafel segments of the anodic and cathodic curves were extrapolated to corrosion potential (E_{corr}) to obtain the corrosion current densities (i_{corr}). In each measurement, a fresh working electrode was used. Several runs were performed for each measurement to obtain reproducible data.

2. 2. Computational Details

The use of quantum chemical calculations has become popular for screening new potential corrosion inhibitors [17]. Theoretical calculations were carried out at density functional theory (DFT) level using the 6-31G (d, p) basis set for all atoms with Gaussian 03 program package. Electronic properties such as highest occupied molecular orbital (HOMO) energy, lowest unoccupied molecular orbital (LUMO) energy and frontier molecular orbital coefficients have been calculated. The molecular sketches of all compounds were drawn using Gauss View 03 [18]. The natural bond orbital (NBO) analysis, suggested by Reed et al. [19, 20], was applied to determine the atomic charges.

3. RESULTS AND DISCUSSION

3. 1. Potentiodynamic Polarization Studies

Polarization measurements were carried out to get information regarding the kinetics of anodic and cathodic reactions. The potentiodynamic polarization curves for SS in 0.5 M H_2SO_4 solution in the absence and presence of different concentrations of the inhibitor molecules are shown in Fig. 1. The values of electrochemical kinetic parameters such as corrosion potential (Ecorr), corrosion current (Icorr) and Tafel slopes, determined from these by extrapolation method, are listed in Table 1. In corrosion, quantitative information on corrosion currents and corrosion potentials can be extracted from

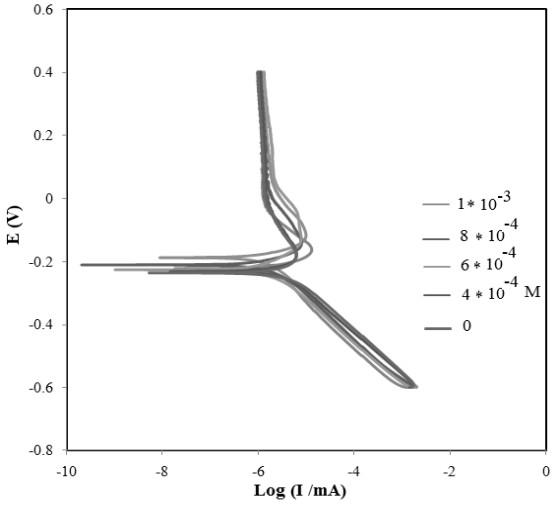

Fig. 1. Potentiodynamic polarisation curves of SS in 0.5 M H_2SO_4 solution in the absence and presence of various concentrations of the NBTA.

[DOI: 10.22068/ijmse.13.3.19]

Table 1. Corrosion parameters obtained from Tafel polarisation curves of SS in 0.5M H_2SO_4 in the absence and presence of different concentrations of NBTA at 298 K.

No.	Inhi. Con.	Ba(v/decade)	Bc(v/dedade)	I(uA)	E(v)	CR(mpy)
SS1	0	0.61	0.14	12.76	-0.22	5.25
SS2	0.0001	0.16	0.14	5.78	-0.24	2.38
SS3	0.0002	0.16	0.14	3.71	-0.23	1.53
SS4	0.0004	0.17	0.14	2.5	-0.22	1.03
SS5	0.0006	0.09	0.14	2.22	-0.21	0.913
SS6	0.0008	0.04	0.16	2.21	-0.22	0.912
SS7	0.001	0.06	0.15	1.73	-0.18	0.711

the slope of the curves, using the Stern-Geary equation, as follows [21]:

$$i_{corr} = \frac{1}{2.303R_p}\left(\frac{\beta_a \times \beta_c}{\beta_a + \beta_c}\right) \quad (1)$$

i_{corr} is the corrosion current density in Amps/cm^2; R_p is the corrosion resistance in ohms cm^2; β_a is the anodic Tafel slope in Volts/decade or mV/decade of current density; β_c is the cathodic Tafel slope in Volts/decade or mV/decade of current density; the quantity, $\frac{\beta_a \times \beta_c}{\beta_a + \beta_c}$, is referred to as the Tafel constant. The corrosion inhibition efficiency was calculated using the relation:

$$\eta(\%) = 100\left(\frac{i^*_{corr} - i_{corr}}{i^*_{corr}}\right) \quad (2)$$

where $i_{corr}{}^*$ and i_{corr} are uninhibited and inhibited corrosion current densities, respectively, determined by extrapolation of Tafel lines in the corrosion potential. The corrosion rates ν (mm year^{-1}) from polarization were calculated using the following Equation:

$$\upsilon = \frac{i_{corr} \times t \times M}{F \times S \times d} \times 10 \quad (3)$$

where t is the time (s), M is the equivalent molar weight of working electrode (g mol^{-1}), F is Faraday constant (96500 °C. mol^{-1}), S is the surface area of electrode, d is the density of iron and the constant 10 is used to convert the unit cm to mm. The results are presented in table 1. The inhibitor molecule first adsorbs on the SS surface and blocks the available reaction sites. As the concentration of the inhibitor increases, the linear polarization resistance increases and corrosion Rate (CR) decreases. The surface coverage increases with the inhibitor concentration and the formation of inhibitor film on the SS surface reduces the active surface area available for the attack of the corrosive medium and delays hydrogen evolution and metal dissolution [22]. In the cathodic domain, as seen in table 1, the values of βc show small changes with increasing inhibitor concentration, which indicates that the NBTA is adsorbed on the metal surface and the addition of the inhibitor hinders the acid attack on the SS electrode. In anodic domain, the value of βa decreases with the presence of NBTA. The shift in the anodic Tafel slope βa might be attributed to the modification of anodic dissolution process due to the inhibitor modules adsorption on the active sites. Compared to the absence of NBTA, the anodic curves of the working electrode in the acidic solution containing the NBTA clearly shifted to the direction of current reduction, as it could be observed from these polarization results; the

[DOI: 10.22068/ijmse.13.3.19]

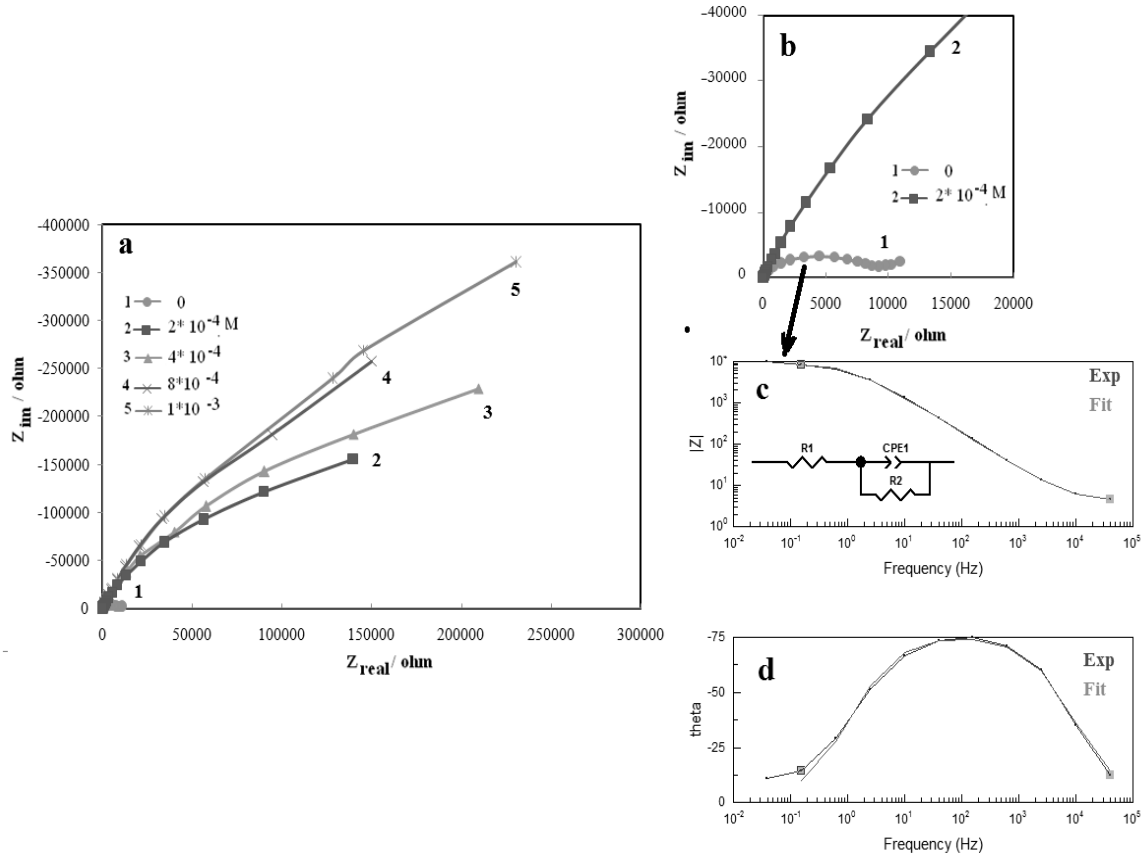

Fig. 2. (a, b) Nyquist plots of SS in 0.5 M H_2SO_4 solution containing different concentrations of the NBTA in different magnification . (c) Electrical equivalent circuit used for fitting.

inhibition efficiency increased with inhibitor concentration.

3. 2. Electrochemical Impedance Spectroscopy

Electrochemical impedance spectroscopy is one of the best techniques for analyzing the properties of conducting polymer electrodes and charge transfer mechanism in the electrolyte/electrode interface. This has been broadly discussed in the literature using a variety of theoretical models [23-27]. Impedance measurements were performed under potentiostatic conditions after 1 h of immersion. Nyquist plots of uninhibited and inhibited solutions containing different concentrations of inhibitor molecules were performed over the frequency range from 100 kHz to 100 mHz and are shown in Fig. 2. The similarity in the shapes of these graphs throughout the experiment indicates that the addition of inhibitor molecules does not cause any noticeable change in the corrosion mechanism [22]. The Nyquist diagrams show one capacitive loop at high frequencies. The capacitive loop at high frequencies represents the phenomenon associated with the electrical double layer. The above impedance diagrams (Nyquist) contain depressed semicircles with the centre under the real axis. Such behavior is characteristic of solid electrodes and often referred to as frequency dispersion, attributed to different physical phenomena such as roughness, inhomogeneities of the solid surfaces, impurities, grain boundaries, and distribution of surface active sites. The ideal capacitive behavior is not observed in this case and hence a constant phase element CPE is introduced in the circuit to give a more accurate

[DOI: 10.22068/ijmse.13.3.19]

fit [28-30]. Obviously, the corrosion behavior of SS in acidic solution is in influenced to some extent by mass transport since the Warburg impedance is observed in Nyquist plots. Anodic dissolution of SS dissolution is mass-transport limited and leads to the formation of sulfate compound. However, the diffusion step was ascribed either to sulfate ions transports to the surface or to the transport of formed compound diffusion to the bulk solution. The mechanism of corrosion remains unaffected during the addition of inhibitor molecules. The simplest equivalent circuit is represented in Fig. 2c, which is a parallel combination of the charge transfer resistance (R_{ct}) and the constant phase element (CPE), both in series with the solution resistance (R_s). The impedance function of a CPE can be represented as:

$$Z_{CPE} = Y_0^{-1}(j\omega)^{-n} \quad (4)$$

where Y_0 is the CPE constant, ω is the angular frequency, and n is the CPE exponent, which can be used as a gauge of the heterogeneity or roughness of the surface [25-31]. W element in equivalent circuit presents Warburg impedance. In the present work, the value of n has a tendency to decrease with increasing inhibitor concentration, which may be attributed to the increase of inhibitor concentration resulted in the increasing surface roughness. For a circuit including a CPE, the C_{dl} could be calculated from CPE parameter values Y_0 and n using the expression [22]:

$$C_{dl} = Y_0 (\omega_m'')^{n} \quad (5)$$

where C_{dl} is the double layer capacitance and ω_m'' is the frequency at which the imaginary part of the impedance has a maximum. As seen in table 2, the double layer capacitance (C_{dl}) decreases with increase in concentration. This can be attributed to the gradual replacement of water molecules by the adsorption of the organic molecules at metal/solution interface, which is leading to a protective film on metal surface. In addition, the more the inhibitor is adsorbed, the more the thickness of the barrier layer increases according to the expression of the Helmholtz model [32]:

$$C_{dl} = \frac{\varepsilon\varepsilon_0 A}{d} \quad (6)$$

where d is the thickness of the protective layer, e is the dielectric constant of the medium, ε_0 is the

Table 2. Impedance parameters for the corrosion of SS in 0.5M H_2SO_4 containing different concentration of NBTA at 298 K.

Concentration x (M)	R_s (Ω)	n	R_{ct} (kΩ)	IE%
0	4.17	0.88	7.81	
2.0×10^{-4}	7.65	0.85	347.70	97.75
4.0×10^{-4}	14.12	0.84	413.50	98.11
6.0×10^{-4}	16.65	0.84	587.87	98.67
8.0×10^{-4}	17.24	0.82	614.39	98.72
1.0×10^{-3}	17.19	0.80	687.14	98.86

[DOI: 10.22068/ijmse.13.3.19]

vacuum permittivity and A is the surface area of the electrode. The equation used for calculating the percentage inhibition efficiency is:

$$\eta(\%) = 100(\frac{R_{ct}^{*} - R_{ct}}{R_{ct}^{*}}) \quad (7)$$

where R_{ct}^{*} and R_{ct} are values of the charge transfer resistance observed in the presence and absence of inhibitor molecules. Impedance parameters are summarized in table 2. The results obtained from the EIS technique in acidic solution were in good agreement with those obtained from the polarization method. As observed in table 2, the adsorption of NBTA molecules on SS surface modifies the interface between the corrosive medium and metal surface and decreases its electrical capacity. The increase in Rct values with increase in NBTAconcentration can be interpreted as the formation of an insulated adsorption layer. At the highest inhibitor concentration of 10^{-3} mol/L, the inhibition efficiency markedly increases and reaches 98.86%. Thus, it can be deduced that NBTA has a clear role in metal protection at the concentration of 10^{-3} M.

3. 4. Adsorption Isotherms

The adsorption of an organic adsorbate at metal/solution interface can be presented as a substitution adsorption process between the organic molecules in aqueous solution, (Org_{aq}), and the water molecules on metallic surface, (H_2O_{ads}) Org_{aq}

$$Org_{aq} + XH_2O_{ads} \leftrightarrow Org_{ads} + XH_2O_{aq} \quad (8)$$

where X, the size ratio, is the number of water molecules displaced by one molecule of organic inhibitor. X is assumed to be independent of coverage or charge on the electrode [33]. Basic information on the interaction between the inhibitors and the steel surface is provided by the adsorption isotherm. The degree of surface coverage, θ, at different inhibitor concentrations in 0.5 M H_2SO_4 (θ = IE(%)/100) at 25 °C. The plot of C/θ against inhibitor concentration, C, displayed a straight line for the tested inhibitor (Fig. 3). The linear plot clearly revealed that the surface adsorption process of NBTA on the SS surface obeys the Langmuir isotherm. Likewise, it suggests that an adsorption process occurs, which can be expressed as follows [34]:

$$\frac{C}{\theta} = \frac{1}{K_{ads}} + C \quad (9)$$

where K_{ads} is the equilibrium constant of the adsorption process. Free energy of adsorption

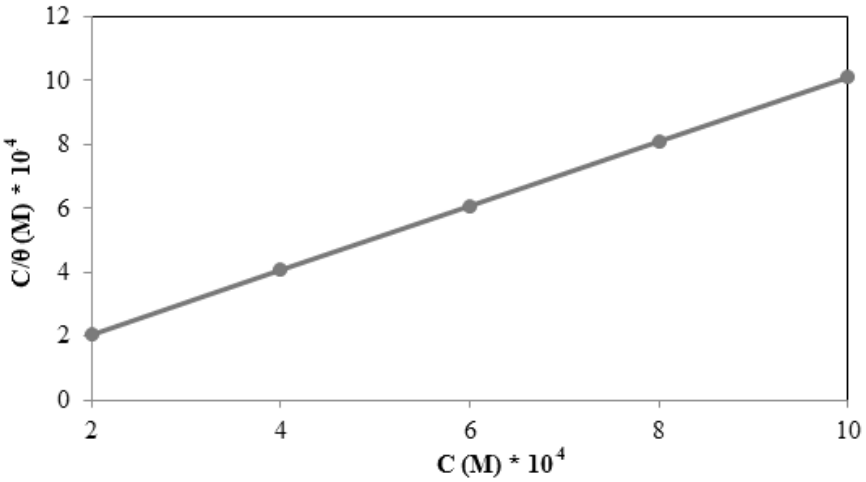

Fig. 3. Langmuir adsorption plot for SS in 0.5 M H_2SO_4 containing different concentrations of NBTA.

[DOI: 10.22068/ijmse.13.3.19]

(ΔG_{ads}) can be calculated by Eq. (10). The numeral of 55.5 is the molar concentration of water in the solution:

$$K_{ads} = \frac{1}{55.5}\exp(\frac{-\Delta G^{0}_{ads}}{RT}) \quad (10)$$

The value of ΔG^0 ads for adsorption of NBTA was found to be -7.88 kJ mol^{-1}. The negative value of ΔG^0 ads suggests that NBTA is spontaneously adsorbed on the SS surface. Literature survey reveals that the values of ΔG^0 ads around -20 kJ mol^{-1} or lower are consistent with the electrostatic interaction between the charged molecules and the charged metal (physical adsorption) [35]. The adsorption of an inhibitor on the metal surface can occur on the basis of donor–acceptor interactions between the p-electrons of the heterocyclic compound and the vacant d-orbitals of the metal surface atoms. Therefore, the energies of the frontier orbitals should be considered. Energy of LUMO shows the ability of the molecule to receive charge when attacked by electron pair donors, even as the energy of HOMO to donate the charge when attached by electron seeking reagents. As the energy gap between the frontier orbitals gets

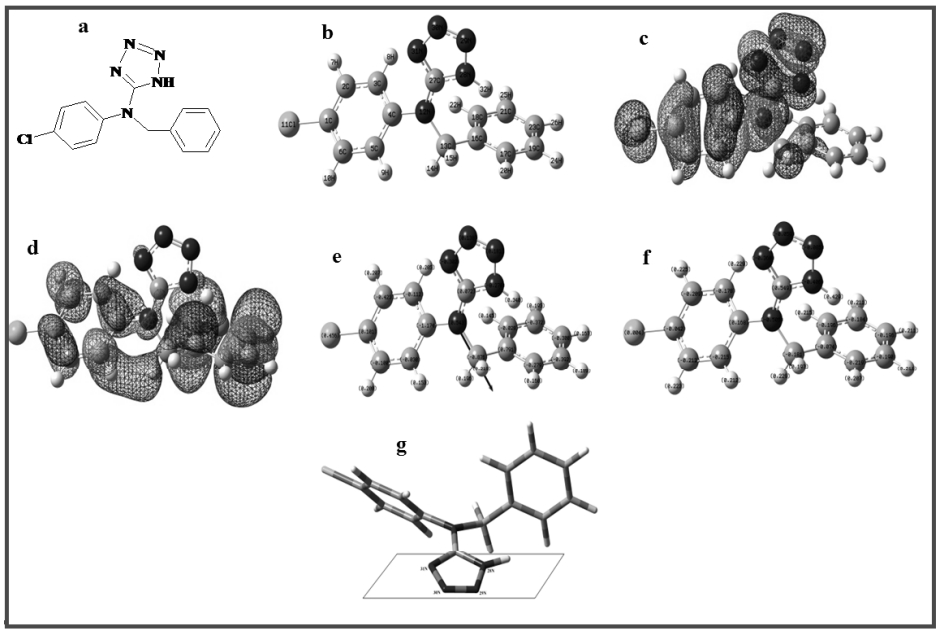

Fig. 4. (a) Structure of NBTA; (b) Optimized molecular structure of NBTA, H atoms have been omitted for clarity; (c) The highest occupied molecular orbital (HOMO) of NBTA; (d) The lowest unoccupied molecular orbital (LUMO) of NBtA; (e) Muliken charge population analysis and vector of dipole moment of NBTA; (f) Natural charge population analysis of NBTA and (g) The schematic representation of the adsorption behavior of NBTA on the surface of the SS.

Table 3. Orbital energies for HOMO, LUMO, HOMO-LUMO gap energy (ΔE) and dipole moment (μ) of Compound in the gaseous phase. All quantum chemical parameters calculated at DFT level using the 6-31G(d,p) basis set.

Compound	phase	E_{HOMO}(ev)	E_{LUMO}(ev)	ΔE(ev)	μ(D)
NBTA	G	-6.395	-1.396	4.999	7.3769
	A	-6.496	-1.153	5.343	9.6801

[DOI: 10.22068/ijmse.13.3.19]

Table 4. Electronegativity (χ), global hardness (η) and proportion of electrons transferred (ΔN) of NBTA.

Compound	phase	χ	η	ΔN
NBTA	G	3.895	2.499	0.621
	A	3.824	2.671	0.594

Table 5. Muliken and Natural Charges (e) for atoms in NBTA.

NBTA	Muliken	Natural
12N	0.543	-0.505
28N	-0.278	-0.406
29N	0.181	-0.085
30N	0.138	-0.059
31N	-0.302	-0.368

smaller, the interactions between the reacting species strengthen [36]. In this regard, the electronic properties such as highest occupied molecular orbital (HOMO) energy, lowest unoccupied molecular orbital (LUMO) energy and frontier molecular orbital coefficients have been calculated for prepared inhibitor. The natural bond orbital (NBO) analysis was applied to determine the atomic charges. Results are presented in figure 4 and tables 3, 4, 5. According to the results, HOMO location in the NBTA molecule is mostly distributed in the vicinity of the nitrogen, oxygen atoms. This indicates the reactive sites of the interaction between NBTA and the SS surface. Mulliken population analysis, presented in figure 4e, is further evidence for the interaction between SS surface and inhibitor active sites. It is clear from figure 4 that the nitrogen atoms of NBTA have considerable excess of negative charge than other atoms. Thus, the adsorption of NBTA as a neutral molecule on the metal surface can occur directly involving the displacement of water molecules from the metal surface and sharing of electrons between the nitrogen atoms and the metal surface. It should be noted that NBTA adsorbs mainly through electrostatic interactions between the positively charged nitrogen atom (since acidic solution can protonate the nitrogen atoms of NBTA and the negatively charged metal surface (physisorption) as evident in the value of ΔG^0_{ads} obtained.

4. CONCLUSION

In the case of NBTA as a corrosion inhibitor for stailess steel in acidic solution , the results of potentiodynamic polarization, electrochemical impedance spectroscopy and quantum chemical analysis was studied in this work. The following points can be emphasized:

1. The potentiodynamic polarization revealed NBTA as a mixed-type corrosion inhibitor with a predominantly anodic action.
2. The results of quantum chemical analysis supported those from the electrochemical measurements relating to the effectiveness of the inhibitor.
3. The nitrogen atoms of NBTA have considerable excess of negative charge than other atoms. Thus, the adsorption of NBTA as a neutral molecule on the metal surface can occur directly involving the displacement of water molecules from the metal surface and sharing of electrons between the nitrogen atoms and the metal surface.
4. The adsorption of DAT on the surface was found to be in accordance with the Langmuir isotherm. By taking advantage of this isotherm, the adsorption process was suggested to take place through electrostatic interaction (physisorption) between inhibitor and iron.

5. ACKNOWLEDGEMENTS

We gratefully acknowledge the support of this work by Qom University Research Council.

REFERENCES

1. Negm, N., Elkholy, Y., Zahran, M. and Tawfik, S., “Corrosion Inhibition Efficiency and Surface Activity of Benzothiazol-3-ium Cationic Schiff Base Derivatives in Hydrochloric Acid”. Corros. Sci., 2010, 52,

[DOI: 10.22068/ijmse.13.3.19]

3523-36.
2. Wang, X., Yang, H. and Wang, F., "An Investigation of Benzimidazole Derivative as Corrosion Inhibitor for Mild Steel in Different Concentration HCl Solutions". Corros. Sci., 2011, 53, 113-21.
3. Döner, A., Solmaz, R., Özcan, M. and Kardaş, G., "Experimental and Theoretical Studies of Thiazoles as Corrosion Inhibitors for Mild Steel in Sulphuric Acid Solution". Corros. Sci., 2011, 53, 2902-13.
4. Markhali, B., Naderi, R., Mahdavian, M., Sayebani, M. and Arman, S., "Electrochemical Impedance Spectroscopy and Electrochemical Noise Measurements as Tools to Evaluate Corrosion Inhibition of Azole Compounds on Stainless Steel in Acidic Media". Corros. Sci., 2013, 75, 269-79.
5. Rochdi, A., Kassou, O., Dkhireche, N., Touir, R., El Bakri, M., Touhami, M. E., Sfaira, M., Mernari, B. and Hammouti, B., "Inhibitive Properties of 2,5-bis(n-methylphenyl)-1,3,4-oxadiazole and Biocide on Corrosion, Biocorrosion and Scaling Controls of Brass in Simulated Cooling Water". Corros. Sci., 2014, 80, 442-52.
6. Finšgar, M. and Merl, D. K., "An Electrochemical, Long-Term Immersion, and XPS Study of 2-mercaptobenzothiazole as a Copper Corrosion Iinhibitor in Chloride Solution". Corros. Sci., 2014, 83, 164-75.
7. Zheludkevich, M., Yasakau, K., Poznyak, S. and Ferreira, M., "Triazole and Thiazole Derivatives as Corrosion Inhibitors for AA2024 Aluminium Alloy". Corros. Sci., 2005, 47, 3368-83.
8. Obot, I., Obi-Egbedi, N. and Umoren, S., "The Synergistic Inhibitive Effect and Some Quantum Chemical Parameters of 2, 3-diaminonaphthalene and Iodide Ions on the Hydrochloric Acid Corrosion of Aluminium". Corros. Sci., 2009, 51, 276-82.
9. Ehsani, A., Mahjani, M. G., Moshrefi, R., Mostaanzadeh, H. and Shayeh, J. S., "Electrochemical and DFT Study on the Inhibition of 316L Stainless Steel Corrosion in Acidic Medium by 1-(4-nitrophenyl)-5-amino-1 H-tetrazole". RSC Adv., 2014, 4, 20031-7.
10. Ehsani, A., Moshrefi, R., Khodadadi, A. and Yeganeh-Faal, A., "Inhibitory of Newly Synthesized 3-BrPhOXTs on Corrosion of Stainless Steel in Acidic Medium". S. Afr. J. Chem. 2014, 67, 198-202.
11. Ehsani, A., Moshrefi, R. and Ahmadi, M., "Electrochemical Investigation of Inhibitory of New Synthesized 3-(4-Iodophenyl)-2-Imino-2, 3-Dihydrobenzo [d] Oxazol-5-yl 4-Methyl-benzenesulfonate on Corrosion of Stainless Steel in Acidic Medium". J. Electrochem. Sci. Tech., 2015, 6, 7-15.
12. Abboud, Y., Abourriche, A., Saffaj, T., Berrada, M., Charrouf, M., Bennamara, A., Al Himidi, N. and Hannache, H., "2, 3-Quinoxalinedione as a Novel Corrosion Inhibitor for Mild Steel in 1M HCl". Mater. Chem. Phys., 2007, 105, 1-5.
13. Quraishi, M., Rawat, J. and Ajmal, M., "Dithiobiurets: A Novel Class of Acid Corrosion Inhibitors for Mild Steel". J. Appl. Electrochem. 2000, 30, 745-51.
14. Khaled, K. and Amin, M. A., "Corrosion Monitoring of Mild Steel in Sulphuric Acid Solutions in Presence of Some Thiazole Derivatives–Molecular Dynamics", Chemical and Electrochemical Studies. Corros. Sci., 2009, 51, 1964-75.
15. Obot, I. and Obi-Egbedi, N., "2, 3-Diphenylbenzoquinoxaline: A New Corrosion Inhibitor for Mild Steel in Sulphuric Acid". Corros. Sci., 2010, 52, 282-5.
16. Habibi, D., Nasrollahzadeh, M., Sahebekhtiari, H. and Parish, R. V., "Ultrasound-Promoted Synthesis of Novel 2-imino-3-aryl-2, 3-dihydrobenzo[d] oxazol-5-ol 2-iminooxazolidines Derivatives". Tetrahedron., 2013, 69, 3082-7.
17. Kokalj. A., "Is the Analysis of Molecular Electronic Structure of Corrosion Inhibitors Sufficient to Predict the Trend of Their Inhibition Performance". Electrochim. Acta., 2010, 56, 745-55.
18. View G. version 3.0.; Gaussian. Inc: Pittsburgh, PA. 2003.
19. Reed, A. E., Curtiss, L. A. and Weinhold, F., "Intermolecular Interactions from a Natural Bond Orbital, Donor-Acceptor Viewpoint". Chem. Rev., 1988, 88, 899-926.
20. Schelegel, H. B., "Ab Initio Methods in Quantum Chemistry". John Wiley, New York,

[DOI: 10.22068/ijmse.13.3.19]

USA, 1987, 249-86.
21. Moshrefi, R., Mahjani, M. G., Ehsani, A. and Jafarian, M., "A Sstudy of the Galvanic Corrosion of Titanium/L 316 Stainless Steel in Artificial Seawater Using Electrochemical Noise (EN) Measurements and Electrochemical Impedance Spectroscopy (EIS)". Anti- Corros. Method M., 2011, 58, 250-7.
22. Tao, Z., Zhang, S., Li, W. and Hou, B., "Adsorption and Inhibitory Mechanism of 1 H-1, 2, 4-triazol-l-yl-methyl-2-(4-chlorophenoxy) acetate on Corrosion of Mild Steel in Acidic Solution". Ind. Eng. Chem. Res. 2011, 50, 6082-8.
23. Ehsani, A., Mahjani, M. G. and Jafarian, M., "Electrochemical Impedance Spectroscopy Study on Intercalation and Anomalous Diffusion of AlCl4- Ions into Graphite in Basic Molten Salt". Turk. J. Chem., 2011, 35, 735-43.
24. Ehsani, A., Vaziri-Rad, A., Babaei, F. and Shiri, H. M., "Electrosynthesis, Optical Modeling and Electrocatalytic Activity of Ni-MWCNT-PT Nanocomposite Film". Electrochim. Acta., 2015, 159, 140-8.
25. Ehsani, A., Mahjani, M., Jafarian, M. and Naeemy, A., "Electrosynthesis of Polypyrrole Composite Film and Electrocatalytic Oxidation of Ethanol". Electrochim. Acta. 2012, 71, 128-33.
26. Ehsani, A., Mahjani, M. and Jafarian, M., "Electrosynthesis of Poly Ortho Aminophenol Films and Nanoparticles: A Comparative Study". Synth. Met., 2012, 162, 199-204.
27. Ehsani, A., Mahjani, M., Bordbar, M. and Moshrefi, R., "Poly Ortho Aminophenol/TiO_2 Nanocomposite: Electrosynthesis and Characterization". Synth. Met., 2013, 165, 51-5.
28. Shiri, H. M. and Ehsani, A., "A Simple and Innovative Route to Electrosynthesis of Eu_2O_3 Nanoparticles and Its Nanocomposite with P-type Conductive Polymer: Characterisation and Electrochemical Properties". J. Colloid interface. Sci., 2016, 473, 126-31.
29. Torabian, J., Mahjani, M., Shiri, H. M., Ehsani, A. and Shayeh, J. S., "Facile Electrosynthesis, Characterisation and Electrochemical Performance of Poly Ortho Aminophenol/Al5Y3O12 Nanocomposite as a New High Efficient Supercapacitor". RSC Adv., 2016, 6, 41045-52.
30. Hassan H. H., "Perchlorate and Oxygen Reduction During Zn Corrosion in a Neutral Medium". Electrochim. Acta., 2006, 51, 5966-72.
31. Martinez, S., "Inhibitory Mechanism of Mimosa Tannin Using Molecular Modeling and Substitutional Adsorption Isotherms". Mater. Chem. Phys., 2003, 77, 97-102.
32. Hohenberg, P. and Kohn, W., "Density Functional Ttheory". Phys. Rev. B. 1964, 136, 864-76.
33. Obot, I., Obi-Egbedi, N. and Umoren, S., "Antifungal Drugs as Corrosion Inhibitors for Aluminium in 0.1 M HCl". Corros. Sci., 2009, 51, 1868-75.
34. Özcan, M., Karadağ, F. and Dehri, I., "Interfacial Behavior of Cysteine between Mild Steel and Sulfuric Acid as Corrosion Inhibitor". Acta Phys. Chim. Sin., 2008, 24, 1387-92.

[DOI: 10.22068/ijmse.13.3.19]